Inversion kinematics at deep-seated gravity slope deformations: A paleoseismological perspective

Federico Pasquarè Mariotto[1], Alessandro Tibaldi[2]

[1] {Department of Theoretical and Applied Sciences, Insubria University, Varese, Italy}

[2] {Department of Earth and Environmental Sciences, University of Milan-Bicocca, Milan, Italy}

Correspondence to:

Alessandro Tibaldi, Department of Earth and Environmental Sciences, University of Milan-Bicocca, Milan, Italy. E-mail: alessandro.tibaldi@unimib.it, tel. +39 0264482052, fax +39 0264482073

Abstract

We compare data from three deep-seated gravity slope deformations (DSGSDs) where paleoseismological techniques were applied in artificial trenches. At all trenches, located in metamorphic rocks of the Italian Alps, there is evidence of extensional deformation given by normal movements along slip planes dipping downhill or uphill, and/or fissures, as expected in gravitational failure. However, we document and illustrate - with the aid of trenching - the evidence of reverse movements. The reverse slips occurred mostly along the same planes along which normal slip occurred, and produced drag folds in unconsolidated Holocene sediments as well as the superimposition of substrate rocks on Holocene sediments. The studied trenches indicate that reverse slip might occur not only at the toe portions of DSGSDs, but also in their central-upper portions. When the age relationships between the two deformation kinematics can be sorted out, they clearly indicate that reverse slips postdate normal ones. Our data suggest that during the development of long-lived DSGSDs, inversion kinematics may occur in different sectors of the unstable rock mass. The inversion is interpreted as either due to locking of the frontal blocks of a DSGSD, or the relative decrease in the rate of downward movement in the frontal blocks with respect to the rear blocks.

Eliminato: Since

Eliminato: at

Eliminato: are located in different positions with respect to the slope affected by the DSGSD, it is possible to suggest that reverse slip might occur both at the toe portions of DSGSDs and in

1 Introduction

Deep-seated gravitational slope deformations (DSGSDs) are ten to hundred meter-thick rock masses, which can involve the whole slope of a mountain and are affected by gravitational instability (Zischinsky 1966; Nemcok 1972; Radbruch-Hall et al. 1977; Savage and Varnes 1987). These phenomena have been intensively studied by several authors in terms of their geomorphological features (Mahr 1977; Dramis and Sorriso-Valvo 1994; Tibaldi and Viviani 1999; Rohn et al. 2004), geotechnical properties (Braathen et al. 2004; Pellegrino and Prestininzi 2007), through numerical modelling (Forlati et al. 2001; Hürlimann et al. 2006; Apuani et al. 2013), analogue modelling (Chemenda et al. 2005; Bachmann et al. 2009), interferometry (Tarchi et al. 2003; Antonello et al. 2004; Saroli et al. 2005), structural methods (review in Stead and Wolter 2015), and geophysical methods (Ferrucci et al. 2000; Meric et al. 2005; Pánek et al. 2009). In order to improve the hazard assessment of DSGSDs, the reconstruction of their kinematics is of paramount importance to gain a better knowledge of their evolution, expected ground deformation, and inner workings. This is usually achieved thanks to in-situ instrumentation and interferometric techniques designed to analyse active structures. However, the above types of approach are applicable to slopes subjected to medium-to-high deformation rates (in the order of mm/yr to cm/yr), whereas in the case of extremely slow DSGSDs, interferometric techniques might not be a suitable option. At presently inactive DSGSDs, only trenching methods can be used to asses the age of the latest movements. Above all, it has been proven that DSGSD deformations develop not only as a consequence of creeping and progressive deformation (Genevois and Tecca 1984; McCalpin and Irvine 1995; Evans and Clague 2003), but also through episodic movements (Beget 1985; Thompson et al. 1997; McCalpin 1999; McCalpin and Hart 2003; Tibaldi et al. 2004; Gutiérrez-Santolalla et al. 2005). Since DSGSDs can move through episodic movements, interleaved by periods marked by very low activity or even inactivity, an approach based upon in-situ instruments and interferometric techniques is not always reliable enough to look into the behaviour of slope deformation.

In recent years, paleoseismological techniques by means of artificial trenching have begun to be applied to DSGSDs (McCalpin and Irvine 1995; Tibaldi et al. 1998, 2004; Onida et al. 2000; McCalpin and Hart 2003; Gutiérrez-Santolalla et al. 2005; Tibaldi and Pasquaré 2007; Gutiérrez et al. 2008, 2010, 2015; Agliardi et al. 2009; McCalpin et al. 2011; Pánek et al. 2011; Moro et al. 2012; Gori et al. 2014). By trenching methods, it is possible to reveal the

Eliminato: be not
Eliminato: or non-active
Eliminato: that are presently not active
Eliminato: useful
Eliminato: last
Eliminato: motions
Eliminato: it is not worth employing the aforementioned techniques.
Eliminato: such slope
Eliminato: the above mentioned types of approach are
Eliminato: Trenching
Eliminato: techniques are capable of
Eliminato: ing

presence of shallow deformation structures, measure their geometry and kinematics and define their spatial and chronological characteristics. Given the importance of this methodology to elucidate subsurface structures within DSGSDs, in this work we combine and reinterpret our data coming from trenches excavated across gravitational structures in the Alps (Fig. 1). Such trenches have been selected because they show intriguing similarities to each other. Our interpretations might help shed light into the workings of gravitational structures and contribute to understanding how DSGSDs may develop during time.

2 Case studies

2.1 Mt Scincina, Western Alps

Tibaldi et al. (2004) documented the occurrence of a series of DSGSDs in a hilly region in Piedmont, in the western Italian Alps (Fig. 1). The DSGSD here described, is located near Mt. Scincina and affects a slope extending from 860 m a.s.l. down to 625 m in altitude (Fig. 2). The slope is characterised by slight changes in dip and a few uphill-facing short slopes trending NNW-SSE. Most of the uphill-facing slopes have been filled by sediments that smoothed out the morphology. The uppermost part of the slope terminates against a gentle dipping downhill-facing scarp, mostly trending NNW-SSE, with an arcuate shape in plan view. This scarp is suggested by the asymmetric slope dip of the mountain summit sector that is much steeper along the western flank.

In order to better evaluate the age and kinematics of this DSGSD, an artificial trench located in correspondence of the northern part of the slope is here described. The trench, located at an altitude of 750-760 m and trending N117° (Figs. 2 and 3), shows three main fracture planes that correspond with the contacts between the metamorphic basement (MB) and Quaternary glacial deposits (YQU). The local basement is composed of micaschists belonging to the Scisti dei Laghi Unit (Boriani et al., 1990). In the log performed on the northern trench wall (Fig. 3A), starting from the left (i.e. west) there is a main slip plane (S1) dipping 80° downhill (in the log section the dip is apparent) with well-defined wall contacts and striae. The slip plane strikes N85° and the striae have a pitch of 47-49°W (see also the stereograms in Fig. 3). The plane puts into contact basement metamorphic rocks in the hanging wall block on the northern side of the fracture, with glacial deposits from the Late Glacial Maximum (YQU, dated at 26.5-32.2 ka BP) in the footwall block. This geometry and the striae indicate

Eliminato: allowing
Eliminato: to
Eliminato: ing
Formattato: Tipo di carattere:(Predefinito) Times New Roman
Formattato: Tipo di carattere:(Predefinito) Times New Roman
Eliminato: here
Formattato: Tipo di carattere:(Predefinito) Times New Roman

transpressional kinematics with a subordinate right-lateral component. The right-lateral strike-slip component is quite obvious due to the location of the trench at the northern side of the deforming slope, whereas the reverse motion component is quite uncommon. A fish-eye structure (Fig. 3B) in the metamorphic rocks shows the bending of schistosity along the plane at the contact with unit YQU, consistent with the component of reverse motion. Close to the slip plane, the metamorphic rocks are intensely folded. A few meters away from the plane, the metamorphic rocks are marked by more open folds with axial surfaces dipping at low angles (10–15°) to the NNE. Further east, two, N20°-striking parallel vertical fractures are observed, 1.5 m apart from one another. They put YQU deposits into contact with metamorphic rocks in the form of a fissural structure that suggests an about E-W-trending dilation.

The remaining portions of the DSGSD are characterised by downhill-facing scarps in the upper section of the slope that suggest extensional deformations, and by a bulging of the slope toe.

2.2 Foscagno Pass, Central Alps

In the upper Valtellina region, Central Alps (Italy), near the Foscagno Pass (Figs. 1 and 4), several indications of recent deformation can be individuated. Such morphostructures mostly consist of downhill- and uphill-facing scarps, linear troughs, and double crested ridges, regarded as the effects of a DSGSD. The slope affected by the DSGSD extends from the mountain crest at about 2900 m a.s.l., down to 2260 m at the valley bottom. The total potential volume composing the DSGSD is about 1.5 km^3. Most of the mountain top is affected by a trench several meters to tens of meters wide. The trenches are parallel to the local slope and are bounded by two sub-parallel to parallel mountain crests, up to several meters in height. These structures indicate extensional deformation of the uppermost part of the unstable slope with a NE-SW to ENE-WSW direction of elongation. The central and lower parts of the slope are characterized by three main, well-defined, uphill-facing scarps that strike NW-SE to NNW-SSE, and are from a few tens of meters to 1 km long. These scarps are sub-parallel to the slope contour lines, but have a more rectilinear trace in plan view (Fig. 4). This geometry suggests that the planes along which the motions took place are steeply-dipping or sub-vertical. They cut the metamorphic bedrock as well as some of the surface deposits and glacial landforms attributed to LGM and post-LGM phases by means of radiometric dating (Calderoni et al. 1998) and field evidence (Forcella et al. 1998). The local basement is composed of dominant micaschists. The observed uphill-facing scarps do not

Formattato: Tipo di carattere:(Predefinito) Times New Roman

Eliminato: it is uncommon to have

Formattato: Tipo di carattere:(Predefinito) Times New Roman

Eliminato: parts

Formattato: Tipo di carattere:(Predefinito) Times New Roman

Eliminato: portion

Formattato: Tipo di carattere:(Predefinito) Times New Roman

Eliminato: is

Formattato: Tipo di carattere:(Predefinito) Times New Roman

Formattato: Tipo di carattere:(Predefinito) Times New Roman

Eliminato: here

show, in general, any correlation with rock fabric. We describe hereunder a trench dug across one of the uphill-facing scarps.

The trench was excavated at the toe of the DSGSD, at an altitude of 2320 m (Fig. 4). An analysis of the trench log reveals layers of poorly aggregated sedimentary deposits that rest on the metamorphic basement and are bounded by erosive or slip surfaces (Fig. 5). The lower units (marked as B-C in Fig. 5), limited by a graben-like structure, rest in direct contact with the basement. Such units, dated between 10,975 ys BP and 5065 ys BP, are intensely faulted, hence revealing a late Holocene age of deformation. In units B-C, the bedding is accentuated by textural features and the preferential elongation of pebbles. The alignment of pebbles shows a local bending, which can be correlated with slip planes having different size and kinematics. Downslope (i.e. eastward), three minor slip surfaces occur (S2, S3 and S4), which caused dm-sized normal dislocations through the basement/cover boundary and in the sedimentary layers (see also stereograms in Fig. 5). Upslope (i.e. westward), layers B-C are bent against the main slip plane (S1) that dips steeply in a downhill direction. Further westward (to the left side of Fig. 5), the deposit labeled as "D" can be observed, the lowest portion of which is composed of *in-situ* fractured basement rock that transitions up into a poorly-organized deposit of boulders and pebbles encased in a matrix of clay and fine sand. Deposit D can be interpreted as the accumulation of scree into an open fissure. Moreover, deposit D is bent along plane S1 with a geometry that is consistent with reverse kinematics (see box in Fig. 5). All the above described deposits and slip planes are unconformably covered and sealed by two heterogeneous, lenticular and chaotic debris flow deposits (E and F in Fig. 5).

An interpretation of the above illustrated data, allows to put forward three main phases of deformation: 1) after the emplacement of deposits B-C, a first extensional phase produced the activation of the steeply-dipping slip planes along which normal movements took place, which resulted in a small semi-graben structure; 2) this phase was followed by the formation of a wide sub-vertical open fissure uphill of the semi-graben, which acted as a trap for the infilling of detritus D; 3) an inversion of kinematics occurred along the valley side wall of the previous fissure, and reverse movements developed along surface S1 as suggested by the dragging of layers.

2.3 Bregaglia Valley, Central Alps

The third DSGSD we examined is sited in the Bregaglia Valley (Central Alps, Italy) (Fig. 1) along the tectonic Gruf Line (Tibaldi and Pasquaré 2007). The latter is a zone of intense ductile shearing corresponding to the verticalized tectonic contact between the Tambo nappe - Chiavenna ophiolite complex to the N and the Gruf migmatite complex to the S (Schmid et al. 1996; Berger et al. 1996). The mountain affected by the slope deformation rises at an elevation of 2370 m, and the valley bottom lies at an elevation of 520-630 m (Fig. 6). The DSGSD affects the slope from the valley bottom to a maximum elevation of about 1700 m. The slope dips towards the north, and is interrupted by several downhill- and uphill-facing scarps, each from a few meters to several hundreds meters long. Most of the identified scarps strike E-W, but some strike also WNW-ESE, especially in the northeastern sector of the DSGSD. Two deeply-incised gorges bound the sides of the DSGSD. The rocks cropping out along these valleys are pervasively crushed, with several vertical to sub-vertical planes striking N-S to NW-SE that should correspond to the side walls of the DSGSD. The head of the DSGSD is represented by a northward steeply-dipping scarp that represents the zone of detachment and coincides with the trace of the Gruf Line (Fig. 7B). This area was affected by a strong N-S extensional gravity deformation. The whole DSGSD is broken down into four main blocks, separated by three slip planes dipping at high angle towards the valley floor (i.e. towards the north, Fig. 7), which highlight local strong N-S-directed gravity extensional deformation. The blocks are internally dissected by pervasive, subsidiary, synthetic and antithetic slip planes that indicate more complex local kinematics. The toe of the slope is characterised by a major bulging area that might represent a sector subjected to contractional deformation. The studied DSGSD can be regarded as belonging to the "block slide" type (Varnes 1978) in view of the fact: a) the basal sliding surface is well-defined; b) the movement of the DSGSD has occurred in a mainly translatory fashion; c) internal slip planes break the DSGSD into different blocks; d) "*horst and graben*" type structures are noted near the tip of the gravitational deformation (Fig. 3B).

The trench site is characterised by an ENE-striking, uphill-facing scarp that cuts the bedrock (Figs. 6 and 7 for location). The log of the wall exposed by the artificial trench reveals a series of slide surfaces affecting the bedrock and the sedimentary infill of the depression induced by the uphill-facing scarp (Fig. 8). It is possible to highlight that the deformation of the DSGSD was a multistage one, which developed through decreasing incremental offsets (i.e. older layers were subjected to larger offsets), until very small offsets (a few decimetres) were

Eliminato: suffered

Eliminato: huge

Eliminato: of

produced in the later stages. Above the metamorphic substrate (A) there is a coarse deposit encased in a silty matrix (B) and containing several boulders up to 60 cm in diameter. This deposit, characterized by a quite regular thickness, abruptly abuts against slip plane S3 and is offset by slip plane S4 (see also the stereogram in Fig. 8). These slip planes are steeply dipping uphill (i.e. southward); moreover, S3 merges upward with slip plane S2. Quite a few fragments from deposit B are aligned along S1 and the upper sector of S2, all the way up to a few dm from the topographic surface (small box in Fig. 8B). Above B, deposit C is characterised by several tree fragments, and is overlain by a series of thin, silt and clay deposits (D and E). Layers D and E are folded against slip plane S2, indicating reverse motions. The undeformed and recentmost clay-silt deposit F lies in unconformity above deposit E. The lower stratigraphic unit (B), which was sampled along the slip plane, was dated to AD 400–570, whereas the upper unit (E) was dated to AD 1380–1450 and AD 1300–1370. Dendrochronology age determinations performed on two trunks of alpine larch trees from unit C provided the same year: AD 1523 (Tibaldi and Pasquaré, 2007).

The above illustrated data allows to identify the following evolution: 1) an extensional phase affected the studied sector of the DSGSD as proved by the emplacement of a series of sedimentary units in onlap against an uphill-facing scarp, starting with unit B. The deformation was incremental with the larger offset at unit B along plane S3 and possibly along plane S4; 2) deposit C partially filled the depression and was followed by deposition of units D and E in the interval AD 400-1523; 3) further normal movements have occurred after AD 1523, as witnessed by small normal offsets affecting also deposits C and D, along some of the slip planes (however, it is problematic to quantify them); slip planes S3 and S4 locked; 4) slip plane S2 inverted its kinematics producing the dragging of layers D and E, compatible with reverse motions.

3 Discussion

3.1 Extensional deformation

The paleoseismological analyses illustrated in this work were performed on trenches excavated in different locations of a DSGSD; the Foscagno trench is located in the toe section of the DSGSD, whereas the Scincina and Bregaglia trenches are located in the central-upper part of the slope, at about 2/3 of the length of the DSGSD. All trenches show the presence of

249 extensional deformations: at Bregaglia and Foscagno they are expressed in the form of slip
250 planes dipping downhill or uphill, with normal kinematics. Within the Foscagno and Scincina
251 trenches there is also evidence of formation of extensional fissures along vertical to sub-
252 vertical planes striking normal to the general slope dip. At the Foscagno trench, it has been
253 possible to establish that extensional fissuring developed only after the formation of the first
254 normal slip planes. As a consequence, the Foscagno site suggests that activation of at least a
255 part of a DSGSD can originate from progressive downslope movements of the unstable rock
256 mass along discrete slip planes. Successively, slip locking can occur and extension is released
257 by fissure deformation. The presence of these two types of deformation has been detected also
258 at the Scincina site, although the exposure did not allow to establish the relative chronology of
259 deformation. At other DSGSDs, especially in sedimentary rocks, it has been proposed that,
260 usually, fissuring precedes the development of normal slip planes (e.g. Margielewski and
261 Urban 2003). We stress that caution should be used in generalising the mode of deformation
262 at DSGSDs because, as shown by our data, the steps of development of the rock mass
263 instability may be more complex, depending on several different parameters.

264 Regarding the relations of fissuring vs. normal slip planes with respect to the presence of
265 predisposing mechanical anisotropy, in the Bregaglia Valley study, the upper portion of the
266 DSGSD originated in correspondence of the tectonic Gruf Line (Fig. 7B). Moreover, most of
267 the slip planes of this DSGSD strike in the same trend as the Gruf Line, suggesting that, here,
268 ancient tectonic deformation events produced a preferential rock anisotropy. Gravity
269 reactivated part of these tectonic structures that correspond to the upper vertical to subvertical
270 sections of the DSGSD slip planes. This situation seems to favour the inception and
271 development of slip planes instead of extensional fissuring, as confirmed by the fact that the
272 latter deformation type is not present at the Bregaglia trench site. The dominance of slip
273 planes has also been documented at other trench sites within DSGSDs, such as at Mt.
274 Morrone (Appennines, Italy) (Gori et al. 2014), whose data revealed that the DSGSD initiated
275 after the activation of a dip-slip fault. The activity of this fault resulted in increased local
276 relief, while another close tectonic fault acted as a sliding plane in its surficial portion. The
277 activity of both faults produced structural features and discontinuities that weakened the rock
278 mass and provided preferential sliding zones. A similar situation has been observed also at
279 another DSGSD studied by means of paleoseismological techniques at Mt. Serrone (Central
280 Italy) by Moro et al. (2012). Also in the Carpathian Mountains, Panek et al. (2011) suggested
281 that the spatial coincidence of gravitational morphostructures with an inherited structural

anisotropy represents the evidence of a strong predisposition of the initiation of DSGSDs to be controlled by pre-existing tectonic structures, a characteristic that has been more and more discussed lately (see Stead and Wolter 2015, and references therein).

On the contrary, in the two other trench sites described in this work (Foscagno and Scincina), there exists no geometric relation between gravity structures and regional tectonic structures. This means that pure gravity forces were able to induce rupture of the rocks along planes of shear concentration, independently from the pre-existing rock anisotropy.

3.2 Inversion kinematics

In all the studied trench sites we documented the presence also of reverse kinematics. The reverse motions are expressed by drag folds of the recent sedimentary strata that infilled the previous depressions created by the DSGSD uphill-facing scarps or by extensional fractures. The recent sedimentary strata are folded against the slip planes with a unique geometry. Moreover, at the Foscagno and Scincina trench sites, the substratum rocks are displaced in the hanging wall block above the Holocene sedimentary strata, which compose the footwall block. Finally, also flat clasts are systematically re-oriented along slip planes, a geometry that is compatible with reverse kinematics.

Other different possible causes for these compressional deformations, such as glaciotectonics, have to be ruled out, because the studied drag folds occurred in the late Holocene when glaciers did not cover any longer the studied areas. Moreover, the drag folds developed within protected depressions carved in the slopes, or even at some meters of depth such as at the Foscagno trench. In any case, glaciotectonics could not play any role whatsoever in the observed structural superimposition of metamorphic rocks above Holocene strata, documented at the Scincina trench.

Alternative interpretations in a more strictly structural sense, might be: i) dragging along listric planes, and ii) reverse fault dragging. Regarding point i), it is well known that movements along a fault which is not rectilinear in section view require adaptation of the rock volume in the hanging wall block as a consequence of changing fault dip (Wernicke and Burchfiel 1982; Dula 1991; Higgs et al. 1991; Ruch et al. 2010). In the case of a fault plane whose dip decreases with depth, a roll-over anticline may develop (Fig. 9A). In this case, the bending of the hanging-wall layers develops in correspondence of the greater decrease in fault dip. However, in our case studies this possibility needs to be ruled out as there is no change in

attitude of the slip planes along which the drag folds developed; hence, a geometric adaptation of the hanging-wall layers is not required. In regard to point ii), as can be seen in Figure 9B, usually a normal fault can show fault dragging which is compatible with the sense of shear. Instead, the phenomenon of reverse fault dragging is represented by the possibility that normal faulting was accompanied by an apparent dragging that suggests an opposite sense of slip, i.e. reverse movement (Fig. 9C) (Grasemann et al., 2005). These authors suggested that reverse dragging may stem from perturbation flow induced by fault slip. Material on both sides of the fault is displaced and 'opposing circulation cells' arise on opposite fault sides. This anomalous pattern may develop at the fault center, depending on the angle Θ between the layers and the fault: a correct dragging develops there for low angles (Θ <30–40°), and an "apparent" reverse drag for higher angles. In our studied trenches, we do admit that the angle between the deformed layers and the slip plane is >40°, and thus theoretically "apparent" reverse fault dragging might have occurred. However, the surface condition studied at the trenches is very different from the depth condition analysed in the work of Grasemann et al. (2005). Moreover, the studied bending of layers is observed in the uppermost part of the slip plane, near the tip, and not in the central part of a fault where reverse dragging may occur. We also emphasize that in our case we clearly observed also the superimposition of substrate rocks onto Holocene deposits, which indicate an unambiguous reverse kinematics.

We conclude that our field data suggest that slip planes inherited from a previous phase of extensional deformation, linked to the earlier development of the three studied DSGSDs, were re-activated in the form of reverse kinematics. As far as we know, these are the first artificial trenches that, by means of paleoseismological observations, illustrate the presence of compressional deformations within DSGSDs. Moreover, since our trenches are placed in different positions within the DSGSDs, we also document the possible kinematic inversion with development of reverse slip planes in different parts of the unstable slopes.

At the Foscagno and Bregaglia trenches, since uphill-facing scarps are still present, the reverse offsets were not large enough to nullify the previous normal offsets. At the Scincina site, a morphological scarp is not present in correspondence of the reverse slip plane. This may be due to deletion of previous normal offset by kinematic inversion, or because the latest offset is older than at the other trench sites and thus at Scincina the scarp was eroded away, or a combination of both. In agreement with the latter interpretation, the deformed deposits at

Scincina have an age of 32.2-26.5 ka BP, whereas at the other trenches the deformed deposits are much younger (deformations younger than 5455 yr BP).

Formattato: Tipo di carattere:(Predefinito) Times New Roman

Compressional deformation linked with gravity slope failure is more easily recognized at rockslide avalanches, as described by Shea and van Wyk de Vries (2008). However, such structures are very different from the ones described here, since rockslide avalanches represent deposits produced by the complete failure of a slope rock mass, whereas DSGSDs involve still-in-place rock masses whose movements are orders of magnitude lower than avalanches. Compressional features have been recognized by Braathen et al. (2004) at the surface of slopes affected by large deep-seated instability, such as in the Norwegian mountains. Braathen et al. (2004) described the possibility of the development of extensional structures in the upper part of a DSGSD, linked to low basal friction, and contractional features at the toe expressed by a stacking of blocks by back-thrusting. The contraction part may be due to high friction along the basal surface, or to "ploughing" due to blocking of the toe (Fig. 9D). Braathen et al. (2004) suggested also a more complex scenario with higher parts of the DSGSD under compression due to spatially changing basal friction (Fig. 9E). Anyhow, we need to stress that in the above cases, low angle reverse faults have been consistently observed, differently from what seen in our trenches where slip planes subjected to reverse motions are steeply dipping. Low-angle reverse slip planes and other contractional structures such as folds, have been recognized at the toe of DSGSDs by Mahr and Nemčok (1977), Savage and Varnes (1987), Chigira (1992), Hermann et al. (2000), Baroň et al. (2004), and Hippolyte et al. (2006).

3.3 Mechanisms of overall deformation

The studied DSGSDs show different mechanisms of overall deformation. The Foscagno DSGSD is characterised by a series of parallel, uphill-facing scarps, rectilinear in plan view, and by the presence of a double crest at the mountain top (crest trench) (Fig. 4). These structures are typical of a sackung-type overall deformation mechanism, as illustrated in Figure 10A. After normal slip and fissuring, reverse motions developed here along a slip plane steeply-dipping downhill, suggesting a change in the kinematics and geometry of deformation, as shown in Figure 10B.

The Scincina DSGSD is characterised by an overall amphitheatre morphology with a semicircular head scarp (Fig. 2), and narrowing of the valley bottom compatible with bulging

at the foot of the DSGSD. These morphostructures are more typical of translational movements along downhill-dipping main slip planes (Fig. 10C). The development of transpressional kinematics with a dominant reverse component found at the Scincina trench site suggests locking of the downhill movement of the frontal block with consequent back-thrusting. Back-thrusting has two components of deformation: one of contraction along the slope dip, and one of uplift as indicated by the arrow in Figure 10C. At both the Foscagno and Scincina sites, the block located downhill of the trench (i.e. downhill of the reverse fault) experienced uplift.

The Bregaglia DSGSD is characterised by a well developed system of downhill- and uphill-facing scarps, with main slip planes dipping towards the valley floor and antithetic slip planes, and possibly one or more, well developed planes reaching the valley bottom (block-slide type) (Fig. 10D). However, this architecture does not "explain" the inversion of movement found at the trench site, which is represented by uplift of the block located uphill of the trench (i.e. the block uphill of the reverse fault). This is compatible with an episode of forward-thrusting, either due to the locking of a block in a more frontal position, or to a higher rate of downslope movement of the rear block with rotational movements (Fig. 10E). This may produce the local, reverse reactivation of a previously normal slip plane also at a higher elevation within the DSGSD.

Another possibility for the development of reverse motions during the evolution of a DSGSD is represented by the presence of a main basal slip plane with a complex geometry. The sketch of Figure 10F, which refers to an analogue model developed by McClay and Ellis (1987) for extensional tectonics, is providing just as an example of the complexity of structures that may develop above a multi-curved basal plane, and caution must be used to apply it to real-case DSGSDs. However, this example with a "ramp and flat" type geometry of the basal plane in section view, shows that the hanging-wall block undergoes different deformation during the translation of the rock succession above parts of the basal sliding plane marked by different geometries. The translation above parts of the sliding plane with a downward convex side produces local extension, whereas the translation above parts with an upward convex side produces local compression. During the slip of the DSGSD rock mass, different parts of the rock succession my experience translation across the extensional dominion and then across the compressional dominion. This creates the conditions for inversion of kinematics. The

Eliminato: In t
Eliminato: example
Eliminato: taken
Eliminato: ed
Eliminato: there is a complex
Eliminato: extrapolate
Eliminato:
Eliminato: s of
Eliminato: Anyway
Eliminato: of
Eliminato: . The movements of
Eliminato: above this geometry
Eliminato: suffers
Eliminato: determine the
Eliminato: with
Eliminato: a
Eliminato: y
Eliminato: .

hypothesis that the basal sliding planes of the Bregaglia or the Scincina DSGSDs may be marked by a complex geometry cannot be ruled out.

In regard to the lithology of the involved rock masses, it can be pointed out that the Foscagno and the Scincina DSGSDs are characterised by a quite monotonous succession of micascists, whereas the Bregaglia DSGSDs have more varied lithologies, although all belonging to metamorphic rock types. Although it may be claimed that the presence of different lithotypes at the Bregaglia site is consistent with the more complex structural architecture of this DSGSD, we argue that the amount, orientation and kinematics of the various slip planes of a DSGSD can result from a more complex series of parameters; these may be explained in terms of: i) the presence of slip planes inherited from previous tectonic phases, ii) the amount of gravity deformation and hence the degree of development of the DSGSD, iii) the geometry of the basal main slip plane, iv), the topography, and v) the lithology of the involved rock types.

3.4 Creep versus stick-slip behaviour and related hazard

The hazard posed by DSGSDs can be very different based on their behaviour. The literature suggests that DSGSDs generally evolve with long-term creep movements (e,g. Bisci et al. 1996), although episodic accelerations of deformation can occur (McCalpin and Irvine 1995). A long-lasting creep behaviour represents the lowest level of hazard, since slow damages at infrastructures can be limited to those exactly placed on the boundary zone of the unstable block. This is the case, for example, of the edifices placed along the boundary zone of the DSGSD of the eastern Mt Etna flank (Pernicana fault), and of the pipes and roads crossing it (Groppelli and Tibaldi, 1999). In the case of large sudden offset at a DSGSD, the hazard can be much larger with the possibility of having local very shallow earthquakes due to stick-slip and more diffuse damage to the infrastructures and edifices resting above the sliding block.

The trenches analysed in this work are useful to gain further insight into the evolution of deformation at DSGSDs and to help improving hazard assessment. We also believe that the application of paleoseismological studies with trenches can help to better understand the behaviour of DSGSDs elsewhere. The Scincina and Foscagno trenches show the presence of buried debris wedges developed at the foot of the slip plane scarp. In tectonic contests, debris wedges usually result from the erosion of fault scarps exhumed by coseismic increments of fault offsets (McCalpin 2009, and references therein). The same debris wedges may be, in

Eliminato: like the one illustrated in Figure 10F,
Eliminato: s
Eliminato: the
Eliminato: Even if one might
Eliminato: case
Eliminato: retain
Eliminato: composite
Eliminato:
Eliminato: related mainly
Eliminato: to
Eliminato: ;
Eliminato: ,
Eliminato: to
Eliminato: thus to
Eliminato: ;
Eliminato: , to
Eliminato: ;
Eliminato: ,
Eliminato: to
Eliminato: ,
Eliminato: to

477 turn, offset by successive increments of faulting. The formation of a debris wedge is related to
478 the rapid and localised erosion induced by the creation of an unstable scarp. On the contrary,
479 the slow continuous faulting of the creeping type is usually not accompanied by any debris
480 wedge formation. In case of an uphill-facing scarp, creeping movements may act as a
481 continuous trap for colluvial deposits originated uphill. This geometry, with deposits
482 onlapping the uphill-facing scarp, is more consistent with our observations at the Bregaglia
483 trench, and thus here creeping probably represents the main mechanism of deformation.

484 Instead, data from the Scincina and Foscagno trenches indicate that these DSGSDs moved
485 through sudden increments in movement, which resembles the stick-slip behaviour of tectonic
486 faults. We point out that also in other instances, paleoseismological investigations at trenches
487 showed the presence of debris wedges compatible with a stick-slip behaviour, such as for
488 example at the Mt Serrone DSGSD (Italy) (Moro et al. 2012), and at the Canelles Reservoir
489 DSGSD (Spain) where a sudden slip increment took place in correspondence of a historic
490 earthquake (Gutierrez et al. 2015). At the Mt Morrone DSGSD, Gori et al. (2014) documented
491 a dominant creeping behaviour, punctuated by abrupt gravitational displacements, similarly to
492 several other examples of DSGSDs studied by means of trenches.

493 However, our work suggests more prudence in establishing the creeping behaviour of a
494 DSGSD. In fact, it has to be clarified that the inversion of kinematics along the sliding planes
495 is accompanied by fault scarp enhancement, and thus debris wedge formation, if the uplifting
496 block is located downward with respect to the fault, as in the case of the Scincina and
497 Foscagno trenches. On the contrary, if the uplifting block is located uphill with respect to the
498 normal slip plane with an inverted kinematic, as in the case of the Bregaglia trench, the scarp
499 is subjected to a reduction in height. As a consequence of the above, in the latter case the
500 debris wedge will not form and the possible occurrence of stick-slip motion will not be
501 recorded.

502

503 **4 Conclusions**

504 Through the application of paleoseismological techniques in artificial trenches excavated in
505 different position at three deep-seated gravity slope deformations (DSGSDs) in the Italian
506 Alps, it has been possible to observe that at all trenches there is evidence of extensional
507 deformations, given by normal movements along slip planes dipping downhill or uphill,
508 and/or fissures, as expected in gravitational failure. At one trench, crosscutting relationships

with the deposits indicate that fissure formation postdates the development of steeply-dipping slip planes, suggesting that fissuring does not always precede shear.

Moveover, we illustrated in trenches the evidence of reverse motions. The reverse slips occurred mostly along the same planes that hosted the normal slips, and produced drag folds of unconsolidated Holocene sediments, and superimposition of substrate rocks onto the same sediments. This suggests the possibility of inversion kinematics at DSGSD slip planes. Since we found inversion kinematics at trenches located in different positions with respect to the slope affected by the DSGSD, we also propose that reverse slip might occur both at the toe of slope deformation, as well as in its central-upper sector.

Inversion kinematics may be due either to the effect of locking of frontal blocks of a DSGSD, or to the relative decrease in the rate of downward movement of the frontal blocks with respect to the rear blocks.

Author contribution

F. P. M. studied the Bregaglia Valley trench and elaborated the related description in the manuscript. A. T. studied also the other trenches and described them. Both authors contributed to the discussion and conclusions.

Acknowledgements

This work is dedicated to our teacher, and then colleague and friend Franco Forcella, who introduced us to the study of deep-seated gravity slope deformations. He will always remain in our memory. We acknowledge the precious comments and suggestions on an earlier version of the paper by an anonymous referee and the editor, Andreas Günther.

Eliminato: useful

Eliminato: of one

Eliminato: of

References

Agliardi, F, Crosta, G., Zanchi, A., Ravazzi, C.: Onset and timing of deep-seated gravitational slope deformations in the eastern Alps, Italy, Geomorphology, 103, 113–129, 2009.

Antonello, G., Casagli, N., Farina, P., Leva, D., Nico, G., Sieber, A. J., Tarchi, D.: Ground-based SAR interferometry for monitoring mass movements, Landslides, 1(1), 21-28, 2004.

Apuani, T., Corazzato, C., Merri, A., Tibaldi, A: Understanding Etna flank instability through numerical models, J. Volcanol. Geotherm. Res., 251, 112–126, 2013.

Bachmann, D., Bouissou, S., Chemenda, A.: Analysis of massif fracturing during deep-seated gravitational slope deformation by physical and numerical modelling, Geomorphology, 103, 130-135, 2009.

Baroň, I., Cílek, V., Krejčí, O., Melichar, R., Hubatka, F.: Structure and dynamics of deep-seated slope failures in the Magura Flysch Nappe, outer Western Carpathians (Czech Republic), Nat. Hazard Earth Sys., 4, 549–562, 2004.

Beget, J. E.: Tephrochronology of antislope scarps on an alpine ridge near Glacier Peak, Washington, USA, Arctic Alpine Res., 17, 143–152: 1985.

Berger, A., Rosenberg, C., Schmid, S. M.: Ascent, emplacement and exumation of the Bergell pluton within the Southern steep belt of the Central Alps, Schweiz Miner. Petrog., 76, 357-382, 1996.

Bisci, C., Dramis, F., Sorriso-Valvo, M.: Rock flow (sackung). In: Dikau R, Brunsden D, Schrott L, Ibsen ML (eds) Landslide Recognition, Identification, Movement and Causes, John Wiley and Sons, New York, pp 150-160, 1996.

Boriani A., Giobbi Origoni E., Borghi A., Caironi V.: The evolution of the Serie dei Laghi (Strona-Ceneri and Scisti dei Laghi): the upper component of the Ivrea-Verbano crustal section; Southern Alps, North Italy and Ticino, Switzerland. Tectonophysics, 182, 103-118, 1990.

Braathen, A., Blikra, L. H., Berg, S. S., Karlsen, F.: Rock-slope failures of Norway, type, geometry deformation mechanisms and stability, Norsk Geol. Tidsskkr., 84, 67-88, 2004.

563 Calderoni, G., Guglielmin, M., Tellini, C.: Radiocarbon dating and postglacial evolution,
564 upper Valtellina and Livignese area (Sondrio, Central Italian Alps). Permafrost Periglac., 9,
565 275-284, 1998.

566 Chemenda, A., Bouissou, S., Bachmann, D.: Three-dimensional physical modeling of deep-
567 seated landslides: New technique and first results, J. Geophys. Res.-Earth, doi:
568 10.1029/2004JF000264, 2005.

569 Chigira, M.: Long-term gravitational deformation of rocks by mass rock creep, Eng. Geol.,
570 32, 157–184, 1992.

571 Dramis, F., Sorriso-Valvo, M.: Deep-seated gravitational slope deformations, related
572 landslides and tectonics, Eng. Geol., 38, 231-243, 1994.

573 Dula, Jr., W. F.: Geometric Models of Listric Normal Faults and Rollover Folds, AAPG Bull.,
574 75, 1609-1625, 1991.

575 Evans, S. G., Clague, J. J.: Origin and activity of antislope scarps in the mountains of
576 southwestern British Columbia, Geol. Soc. Am. Abstracts with Programs, 35, 310, 2003.

577 Ferrucci, F., Amelio, M., Sorriso-Valvo, M., Tansi, C.: Seismic prospecting of a slope
578 affected by deep-seated gravitational slope deformation: the Lago Sackung, Calabria, Italy,
579 Eng. Geol., 57, 53-64, 2000.

580 Forcella, F., Onida, M., Tibaldi, A.: Risultati preliminari di un'indagine di tipo
581 paleosismologico applicata allo studio di deformazioni recenti in ambiente alpino, alta
582 Valtellina (Alpi Centrali, Italia), Geol. Insubr., 3, 63-72, 1998.

583 Forlati, F., Gioda, G., Scavia, C.: Finite element analysis of a deep-seated slope deformation,
584 Rock Mech. Rock Eng., 34, 135-159, 2001.

585 Genevois, R., Tecca, P. R.: Alcune considerazioni sulle deformazioni gravitative profonde in
586 argille sovra consolidate, Boll. Soc. Geol. It., 103, 717-729, 1984.

587 Gori, S., Falcucci, E., Dramis, F., Galadini, F., Galli, P., Giaccio, B., Messina, A., Pizzi, P.,
588 Sposato, A., Cosentino, D.: Deep-seated gravitational slope deformation, large-scale rock
589 failure, and active normal faulting along Mt. Morrone (Sulmona basin, Central Italy):
590 Geomorphological and paleoseismological analyses, Geomorphology, 208, 88-101, 2014.

591 Grasemann, B., Martel, S., Passchier, C.: Reverse and normal drag along a fault, J. Struct.
592 Geol., 27, 999-1010, 2005.

Groppelli, G., and Tibaldi, A.: Control of rock rheology on deformation style and slip-rate along the active Pernicana fault, Mt. Etna, Italy, Tectonophysics, 305, 521-537, 1999.

Gutiérrez-Santolalla, F., Acosta, E., Ríos, S., Guerrero, J., Lucha, P.: Geomorphology and geochronology of sackung features (uphill-facing scarps) in the Central Spanish Pyrenees, Geomorphology, 69, 298–314, 2005.

Gutiérrez, F., Ortuño, M., Lucha, P., Guerrero, J., Acosta, E., Coratza, P., Piacentini, D., Soldati, M.: Late Quaternary episodic displacement on a sackung scarp in the central Spanish Pyrenees: Secondary paleoseismic evidence? Geodin. Acta, 21, 187–202, 2008.

Gutiérrez, F., Lucha, P., Galve, J. P.: Reconstructing the geochronological evolution of large landslides by means of the trenching technique in the Yesa Reservoir (Spanish Pyrenees), Geomorphology, 124, 124-136, 2010.

Gutiérrez, F., Linares, R., Roquéc, C., Zarroca, M., Carbonel, D., Rosell, J., Gutiérrez, M.: Large landslides associated with a diapiric fold in Canelles Reservoir (Spanish Pyrenees): Detailed geological–geomorphological mapping, trenching and electrical resistivity imaging, Geomorphology, 241, 224-242, 2015.

Hermann, S. W., Madritsch, G., Rauth, H., Becker, L. P.: Modes and structural conditions of large scale mass movements (Sackungen) on crystalline basement units of the Eastern Alps (Niedere Tauern, Austria), Mitteilungen des Naturwissenschaftlichen Vereines für Steiermark, 130, 31-42, 2000.

Higgs, W. G., Williams, G. D., Powell, C.M.: Evidence for flexural shear folding associated with extensional faults, Geol. Soc. Am. Bull., 103, 710-717, 1991.

Hippolyte, J.-C., Brocard, G., Tardy, M., Nicoud, G., Bourlès, D., Braucher, R., Ménard, G., Souffaché, B.: The recent fault scarps of the Western Alps (France): tectonic surface ruptures or gravitational sackung scarps? A combined mapping, geomorphic, levelling, and 10Be dating approach, Tectonophysics, 418, 255–276, 2006.

Hürlimann, M., Ledesma, A., Corominas, J., Prat, P. C.: The deep-seated slope deformation at Encampadana, Andorra: Representation of morphologic features by numerical modelling, Eng. Geol., 83, 343-357, 2006.

Mahr, T.: Deep-Reaching gravitational deformations of high mountain slopes, Bull. Intern. Assoc. Eng. Geol., 16, 121-127, 1977.

Mahr, T., Nemčok, A.: Deep-seated creep deformation in the crystalline cores of the Tatry Mts, Bull. Intern. Assoc. Eng. Geol., 16, 104–106, 1977.

Margielewski, W., Urban, J.: Crevice-type caves as initial forms of rock landslide development in the Flysch Carpathians, Geomorphology, 54, 325-338, 2003.

McCalpin, J. P.: Criteria for determining the seismic significance of sackungen and other scarplike landforms in mountainous regions. In: Hanson KL, Kelson KI, Angell, MA, Lettis WR (eds) Techniques for Identifying Faults and Determining their Origins, U.S. Nuclear Regulatory Commission, Washington, pp 255–259, 1999.

McCalpin, J. P.: Paleoseismology, 2nd edition, Academic Press, San Diego, 2009.

McCalpin, J. P., and Hart E. W.: Ridge-top spreading features and relationship to earthquakes, San Gabriel Mountain region, southern California. In: E.W. Hart (Ed.), Ridge-Top Spreading in California; Contributions Toward Understanding a Significant Seismic Hazard, California Geological Survey, CD 2003-05, disk 1 of 2, 2003.

McCalpin, J. P., Irvine, J. R.: Sackungen at the Aspen Highlands Ski Area, Pitkin County, Colorado, Environ. Eng. Geosci., 1, 277–290, 1995.

McCalpin, J. P.,, Bruhn, R. L., Pavlis, T. L., Gutierrez, F., Guerrero, J., Lucha, P.: Antislope scarps, gravitational spreading, and tectonic faulting in the western Yakutat microplate, south coastal Alaska, Geosphere, 7, 1143–1158, 2011.

McClay, K. R., Ellis, P. G.: Geometries of extensional fault systems developed in model experiments, Geology, 15, 341-344, 1987.

Meric, O., Garambois, S., Jongmans, D., Wathelet, M., Chatelain, J. L., Vengeon, J. M.: Application of geophysical methods for the investigation of the large gravitational mass movement of Séchilienne, France, Can. Geotech. J., 42, 1105-1115, 2005.

Moro, M., Saroli, M., Gori, S., Falcucci, E., Galadini, F., Messina, P.: The interaction between active normal faulting and large scale gravitational mass movements revealed by paleoseismological techniques: a case study from central Italy, Geomorphology, 151, 164-174, 2012.

Nemcok, A.: Gravitational slope deformation in high mountains. Proceedings of the 24th International Geological Congress, Montreal, 13, 132–141, 1972.

Onida, M., Tibaldi, A., Forcella, F., Galadini, F.: Analysis of deep-seated slope deformations by paleoseismic technique. In: Girard J, Liebman M, Breeds C, Doe T (eds) Proceedings of the Fourth North American Rock Mechanics Symposium, Balkema, Rotterdam, 515–521, 2000.

Pánek, T., Hradecký, J., Minár, J., Hungr, O., and Dušek, R.: Late Holocene catastrophic slope collapse affected by deep-seated gravitational deformation in flysch: Ropice Mountain, Czech Republic, Geomorphology, 103(3), 414-429, 2009.

Pánek, T., Tábořík, P., Klimeš, J., Komárková, V., Hradecký, J., and Šťastný, M.: Deep-seated gravitational slope deformations in the highest parts of the Czech Flysch Carpathians: evolutionary model based on kinematic analysis, electrical imaging and trenching, Geomorphology, 129(1), 92-112, 2011.

Pellegrino, A., Prestininzi, A.: Impact of weathering on the geomechanical properties of rocks along thermal–metamorphic contact belts and morpho-evolutionary processes: The deep-seated gravitational slope deformations of Mt. Granieri–Salincriti (Calabria–Italy), Geomorphology, 87, 176-195, 2007.

Radbruch-Hall, D. H., Varnes, D. J., Colton, R. B.: Gravitational Spreading of steep-sided ridges ("Sackung") in Colorado. Journal of Research of the US Geological Survey, 5, 359-363, 1977.

Rohn, J., Resch, M., Schneider, H., Fernadez-Steeger, T. M., Czurda, K.: Large-scale lateral spreading and related mass movements in the Northern Calcareous Alps, Bull. Eng. Geol. Environ., 63, 71–75, 2004.

Ruch, J., Acocella, V., Storti, F., Neri, M., Pepe, S., Solaro, G., Sansosti, E.: Detachment depth revealed by rollover deformation: An integrated approach at Mount Etna, Geophys. Res. Letts, 37(16), 2010.

Saroli. M., Stramondo, S., Moro, M., Doumaz, F.: Movements detection of deep seated gravitational slope deformations by means of InSAR data and photogeological interpretation: northern Sicily case study, Terra Nova, 17, 35-43, 2005.

Savage, W. Z., Varnes, D. J.: Mechanics of gravitational spreading of steep-sided ridges (sackung), Bull. Intern. Assoc. Engin. Geol., 35, 31-36, 1987.

Schmid, S. M., Berger, A., Davidson, C., Giere, R., Hermann, J., Nievergelt, P., Puschnig, A. R., Rosenberg, C.: The Bergell pluton (southern Switzerland, northern Italy): overview accompanying a geological-tectonic map of the intrusion and surrounding country rocks, Schweiz Miner. Petrog., 76, 329– 355, 1996.

Shea, T., van Wyk de Vries, B.: Structural analysis and analogue modelling of the kinematics and dynamics of rockslide avalanches, Geosphere, 4, 657–686, 2008.

Stead, D., Wolter, A.: A critical review of rock slope failure mechanisms: The importance of structural geology, J. Struct. Geol., 74, 1-23, 2015.

Tarchi, D., Casagli, N., Moretti, S., Leva, D., Sieber, A. J.: Monitoring landslide displacements by using ground‐based synthetic aperture radar interferometry: Application to the Ruinon landslide in the Italian Alps, J. Geophys. Res., Solid Earth, 108(B8), 2003.

Thompson, S. C., Clague, J. J., Evans, S. G.: Holocene activity of the Mt. Currie scarp, Coast Mountains, British Columbia, and implications for its origin, Environ. Eng. Geosci., 3, 329–348, 1997.

Tibaldi, A., Pasquaré, F.: Quaternary deformations along the 'Engadine–Gruf tectonic system', Swiss-Italian Alps, J. Quaternary Sci., 23, 475–487, 2007.

Tibaldi, A., Viviani, C.: Prima individuazione di deformazioni profonde di versante nella Valle Agogna, Brovello-Carpugnino (VB): loro geometria, età e dinamica. Vol. Spec. Studi Geografici e Geologici in Onore di S. Belloni, Genova, 609-630, 1999.

Tibaldi, A., Onida, M., Pasquarè, G., Forcella, F.: Trenching and palaeoseismic researches along Holocene deformation zones in the upper Valtellina region, Central Alps (Italy). 3rd Workshop on Alpine Geological Studies, Oropa-Biella, 29 Sept. - 1 oct. 1997. Quaderni di Geodin. Alpina e Quat., 4, 219-220, 1998.

Tibaldi, A., Rovida, A., Corazzato, C.: A giant deep-seated slope deformation in the Italian Alps studied by paleoseismological and morphometric techniques, Geomorphology, 58, 27–47, 2004.

Varnes, D. J..: Slope movements types and processes. In: Schuster R.L. & Krizek R.J. (eds.), Landslides, Analysis and Control. Natl. Acad. Sci., Washington D.C., Transp. Res. Board, Spec. Rep., 176, 11-33, 1978.

710 Wernicke, B., Burchfiel, B.C.: Modes of extensional tectonics, J. Struct. Geol., 4, 105-115,
711 1982.

712 Zischinsky, U.: On the deformation of high slopes. Proc. 1st Conf. Int. Soc. Rock Mech.,
713 Lisbon, Sect. 2, 179-185, 1966.
714

FIGURE CAPTIONS

Figure 1. Location of the study areas in the context of the Western and Central Italian Alps.

Figure 2. Digital Elevation Model of the area of the Deep-seated Gravitational Slope Deformation (DSGSD) at Mt. Scincina (western Alps, Italy) with location of the trench studied by way of paleoseismological techniques, and trace of the main morphostructures indentified at the DSGSD.

Figure 3. (A) Log of the northern trench wall excavated across the central-upper part of the DSGSD at Mt. Scincina (western Alps, Italy, for location see Fig. 2). Note the superimposition of the substratum metamorphic rocks (MB) onto Late Quaternary deposits (YQU) along reverse oblique slip plane S1. S2 and S3 are extensional fractures filled by YQU deposits. Stereograms (Schmidt's projection, lower hemisphere) show the geometry of slip planes and orientation of the trench. (B) Photo of the reverse oblique fault that puts into contact MB in the hanging-wall block with YQU in the footwall block. (Modified after Tibaldi et al. 2004).

Figure 4. Digital Elevation Model of the area of the DSGSD near the Foscagno Pass (Central Alps, Italy), with location of the trench studied by paleoseismological techniques, and trace of the main Holocene morphostructures of the DSGSD.

Figure 5. Log of the southern trench wall excavated across the lower DSGSD structure near the Foscagno Pass (Central Alps, Italy, see Fig. 4 for location). Inset shows a log of the southern trench wall where the dragging of layers and clasts along the slip plane S1 is consistent with reverse movements. Plane S1 was previously an extensional fracture. Stereograms (Schmidt's projection, lower hemisphere) show the geometry of slip planes and orientation of the trench.

Figure 6. Digital Elevation Model of the area of the Bregaglia Valley DSGSD (Central Alps, Italy), with location of the trench studied by way of paleoseismological techniques, and trace of the main Holocene morphostructures of the DSGSD.

748 Figure 7. (A) Photo of the Bregaglia Valley DSGSD (Central Alps, Italy) studied by
749 paleoseismological techniques and location of the artificial trench. The DSGSD is subdivided
750 into four main blocks by three slip planes steeply dipping toward the valley floor. Arrows
751 indicate the relative block movements. (B*)* Geological-structural section across the DSGSD.
752 The location of the artificial trench of Figure 8 is shown. Trace X-X' of the section in Figure
753 7A (modified after Tibaldi and Pasquaré 2007).
754
755 Figure 8. (A) Photo of a portion of the wall exhumed during the excavation of the artificial
756 trench at the Bregaglia Valley trench and (B) complete log of the same wall. A series of slide
757 surfaces offset the bedrock and the sedimentary infill of the depression induced by the uphill-
758 facing scarp. Note that offset increases with the age of the layers. Absolute dating was
759 obtained by radiocarbon ^{14}C and dendrochronology techniques. Note the dragging of strata
760 along slip plane S2, compatible with a small uplift of the hanging wall block located uphill of
761 the slip planes. Stereogram (Schmidt's projection, lower hemisphere) shows geometry of the
762 slip planes and orientation of the trench. (Modified after Tibaldi and Pasquaré 2007).
763
764 Figure 9. (A) Bending of strata due to adaptation along a listric normal fault (rollover
765 anticline); (B) normal fault with normal bending of layers, coherent with the sense of shear;
766 (C) normal fault with reverse (apparent) sense of shear due to a high angle Θ (B and C
767 redrawn after Grasemann et al. 2005); (D) development of low angle back-thrusts at the toe of
768 a DSGSD; (E) development of low angle back-thrusts and other contractional deformations in
769 different parts of a DSGSD due to spatial changing in friction (D and E modified after
770 Braathen et al. 2004).
771
772 Figure 10. Section views across different models of DSGSDs. (A) Development of
773 extensional structures at a sackung-type of DSGSD; (B) inversion kinematics at a sackung-
774 type of DSGSD; (C) translational type with inversion kinematics due to locking of the toe
775 block; (D) well-developed translational type, or block slide type, with antithetic slip planes;
776 (E) same as D with reverse movements along an uphill-dipping slip plane; (F) development of
777 reverse slip planes above a basal shear with a complex geometry of the "ramp and flat" type
778 (F modified after McClay and Ellis 1987).
779
780

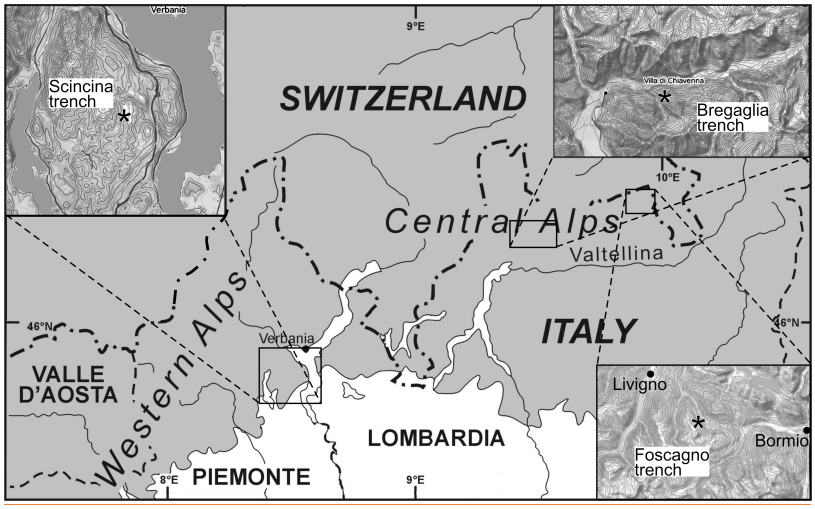

Figure 1.

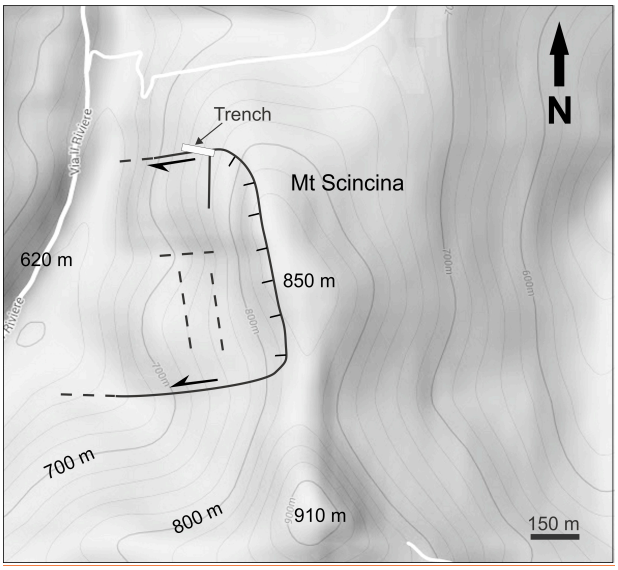

Figure 2.

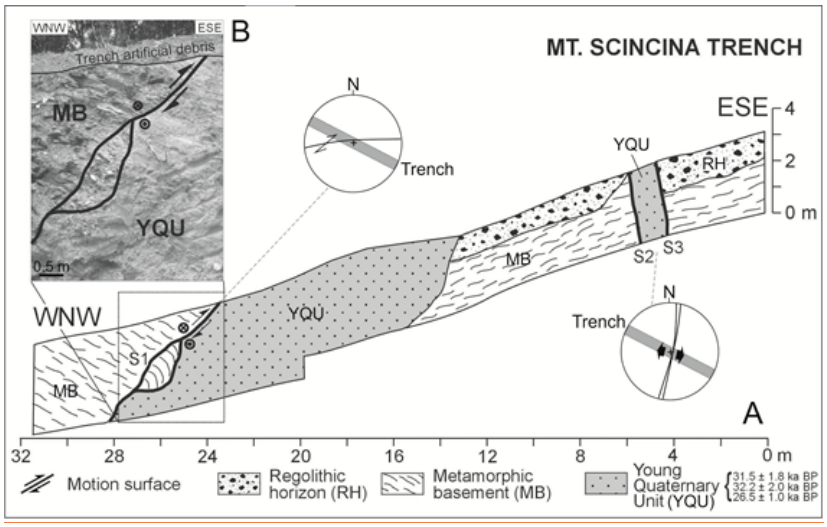
WNW
ESE
Trench artificial debris
MB
YQU
0.5 m
B
MT. SCINCINA TRENCH
N
Trench
ESE
4
2
0 m
YQU
RH
MB
S2
S3
WNW
YQU
S1
MB
N
Trench
A
32
28
24
20
16
12
8
4
0 m
Motion surface
Regolithic horizon (RH)
Metamorphic basement (MB)
Young Quaternary Unit (YQU)
31.5 ± 1.8 ka BP
32.2 ± 2.0 ka BP
26.5 ± 1.0 ka BP

Figure 3.

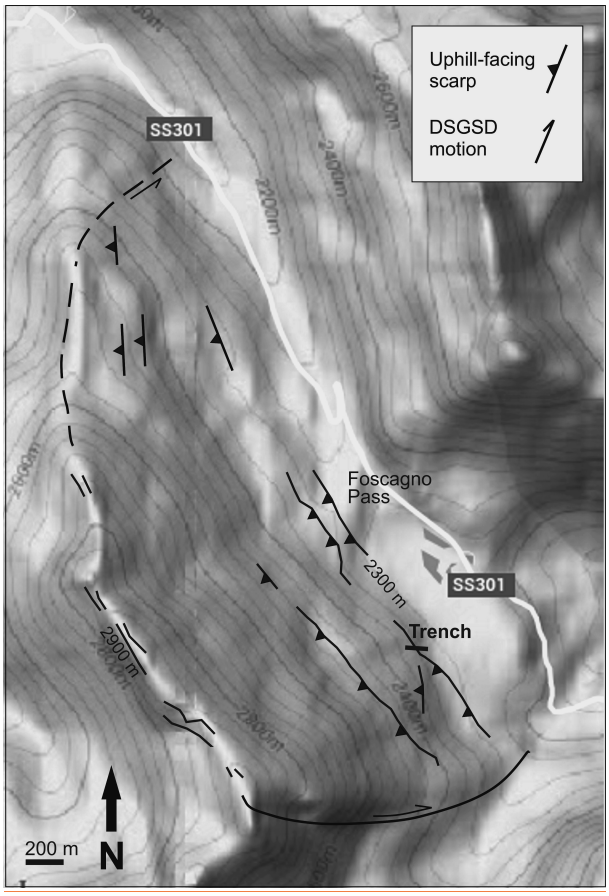
Uphill-facing scarp
DSGSD motion
SS301
2600m
2400m
2200m
2600m
Foscagno Pass
2300 m
SS301
Trench
2900 m
2800m
2400m
200 m
N

Figure 4.

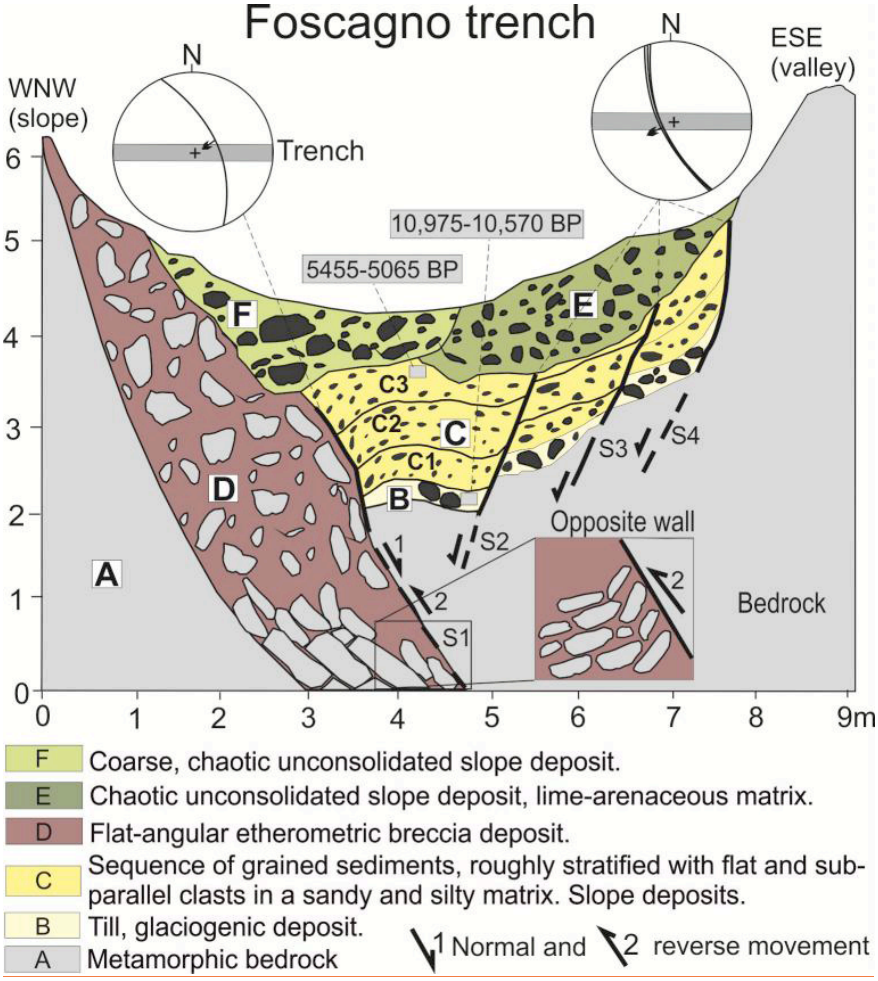
Foscagno trench
N
WNW
(slope)
Trench
N
ESE
(valley)
10,975-10,570 BP
5455-5065 BP
F
E
C3
C2
C1
C
B
D
A
S1
S2
S3
S4
1
2
Opposite wall
Bedrock
0
1
2
3
4
5
6
7
8
9m
F Coarse, chaotic unconsolidated slope deposit.
E Chaotic unconsolidated slope deposit, lime-arenaceous matrix.
D Flat-angular etherometric breccia deposit.
C Sequence of grained sediments, roughly stratified with flat and sub-parallel clasts in a sandy and silty matrix. Slope deposits.
B Till, glaciogenic deposit.
A Metamorphic bedrock
1 Normal and 2 reverse movement

Figure 5.

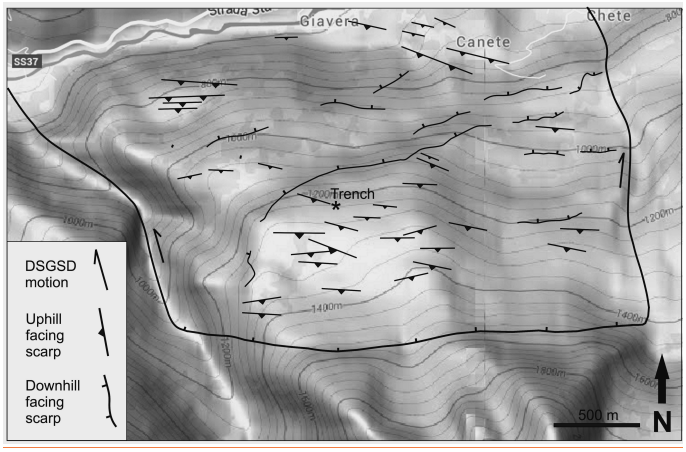
Giavera
Canete
Chete
SS37
Trench
DSGSD motion
Uphill facing scarp
Downhill facing scarp
500 m
N

Figure 6.

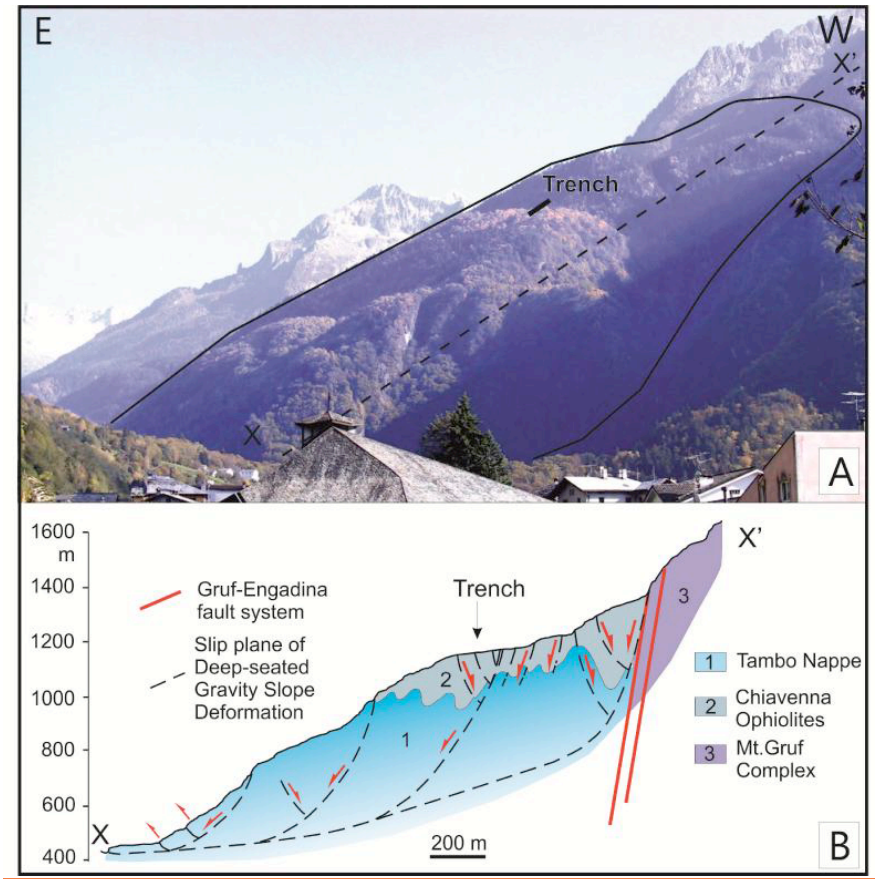
E
W
X'
Trench
X
A
1600
m
1400
1200
1000
800
600
400
Gruf-Engadina
fault system
Slip plane of
Deep-seated
Gravity Slope
Deformation
Trench
X'
X
1
2
3
1 Tambo Nappe
2 Chiavenna
Ophiolites
3 Mt.Gruf
Complex
200 m
B

Figure 7.

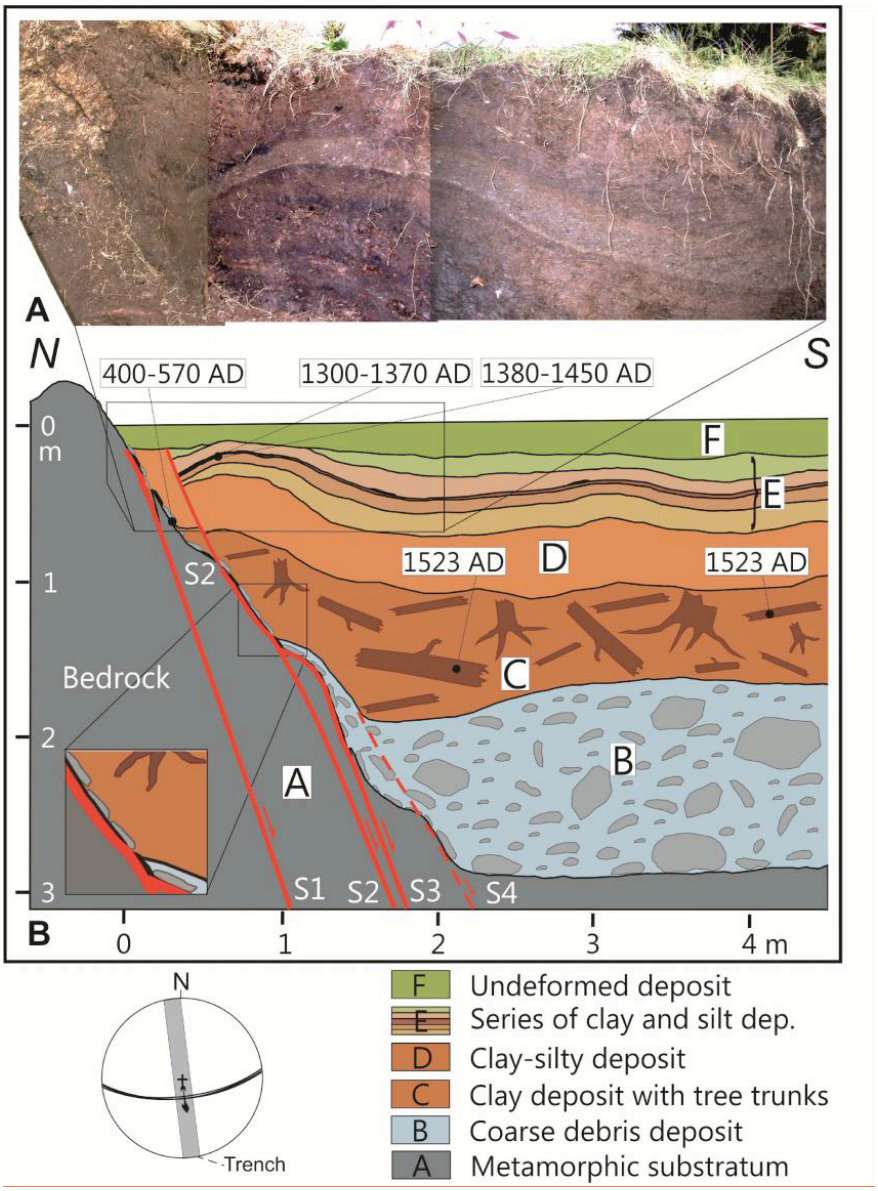
A
N
S
400-570 AD
1300-1370 AD
1380-1450 AD
0 m
1
2
3
F
E
D
1523 AD
1523 AD
S2
Bedrock
C
B
A
S1
S2
S3
S4
B
0
1
2
3
4 m
N
Trench
F Undeformed deposit
E Series of clay and silt dep.
D Clay-silty deposit
C Clay deposit with tree trunks
B Coarse debris deposit
A Metamorphic substratum

Figure 8.

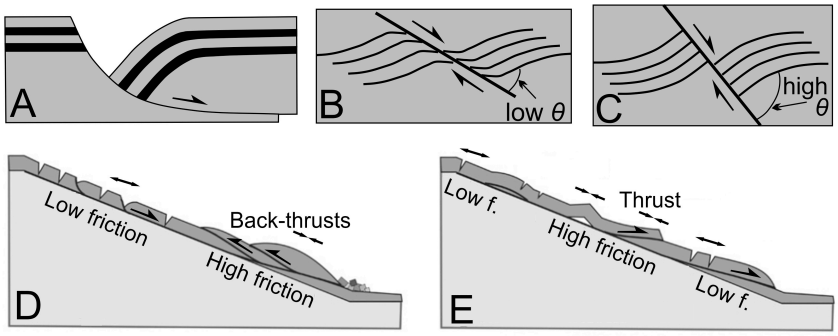
A
B
low θ
C
high θ
Low friction
Back-thrusts
High friction
D
Low f.
Thrust
High friction
Low f.
E

Figure 9.

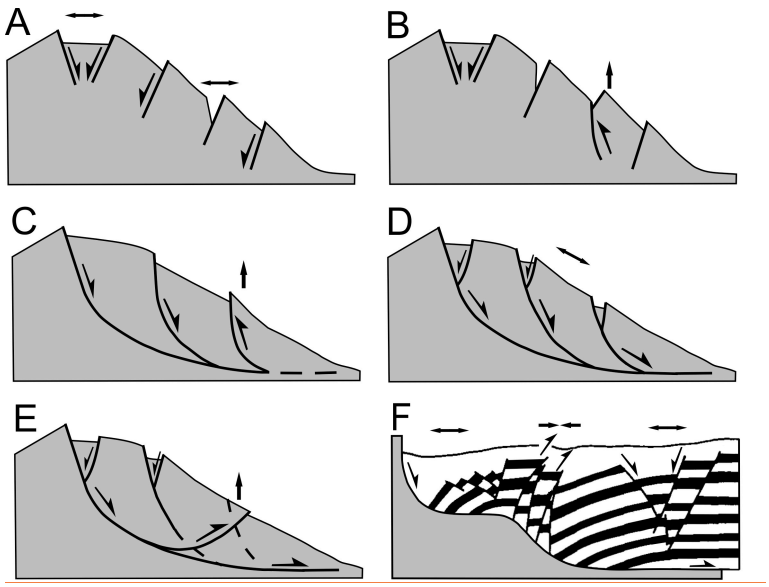
A
B
C
D
E
F

822 Figure 10.
823
824
825
826